mathematics

MDPI

Article

Computational Traveling Wave Solutions of the Nonlinear Rangwala–Rao Model Arising in Electric Field

Mostafa M. A. Khater [1,2,†]

[1] School of Medical Informatics and Engineering, Xuzhou Medical University, 209 Tongshan Road, Xuzhou 221004, China
[2] Department of Basic Science, Obour High Institute for Engineering and Technology, Cairo 11828, Egypt
† This author did all this work.

Abstract: The direct influence of the integrability requirement on mixed derivative nonlinear Schrödinger equations is investigated in this paper. A. Rangwala mathematically formalized these effects in 1990 and dubbed this form the Rangwala–Rao ($\mathcal{RR}$) equation. Our research focuses on innovative soliton wave solutions and their interactions in order to provide a clear picture of the slowly evolving envelope of the electric field and pulse propagation in optical fibers in terms of the dispersion effect. For creating unique solitary wave solutions to the investigated model, three contemporary computational strategies (extended direct (ExD) method, improved F–expansion (ImFE) method, and modified Kudryashov (MKud) method) are employed. These solutions are numerically computed to demonstrate the dynamical behavior of optical fiber pulse propagation. The originality of the paper's findings is proved by comparing our results to previously published results.

Keywords: nonlinear Schrödinger equations; Rangwala–Rao equation; optical fiber; soliton waves

MSC: 35Q60; 35E05; 35C08; 35Q51

Citation: Khater, M.M.A. Computational Traveling Wave Solutions of the Nonlinear Rangwala–Rao Model Arising in Electric Field. *Mathematics* **2022**, *10*, 4658. https://doi.org/10.3390/math10244658

Academic Editor: Yury Shestopalov

Received: 16 October 2022
Accepted: 3 December 2022
Published: 8 December 2022

1. Introduction

Recently, the dynamical and physical characterizations of a system with one degree of freedom have attracted the attention of many mathematicians and physicists [1,2]. This study was given in the presence of a linear restoring force and nonlinear damping of the investigated model [3]. The mathematical model that describes this phenomenon is the Lienard equation formulated by the French physicist Alfred–Marie Liénard [4]. The Lienard equation is given by [5,6]

$$\frac{d^2x}{dt^2} + \Gamma(x)\frac{dx}{dt} + \Xi(x) = 0, \tag{1}$$

where Γ, Ξ are two continuously differentiable functions on $\mathbf{R}$, and, respectively, odd and even functions. A class of classical anharmonic oscillators of Equation (1) can be given by [7]

$$\mathcal{W}'' + r_1\mathcal{W} + r_2\mathcal{W}^3 + r_3\mathcal{W}^5 = 0, \tag{2}$$

where r_1, r_2, r_3 are arbitrary constants; $\mathcal{W} = \mathcal{W}(\chi)$ describes the waves' propagation of the the Alfvén wave with a small non-vanishing wave number. Furthermore, the general form of Equation (2) is given by [8]

$$\mathcal{W}'' + r_1\mathcal{W} + r_2\mathcal{W}^{p+1} + r_3\mathcal{W}^{2p+1} = 0, \tag{3}$$

where $p = 1, 2, 3, \cdots$. These models (2), (3) are beneficial for studying solitary wave solutions of some icons nonlinear evolution equations such as the generalized Ablowitz equa-

tion [9], the generalized Gerdjikov–Ivanov equation [10], the generalized one-dimensional Klein–Gordon equation [11], $\mathcal{RR}$ equation [12], Kundu–Eckhaus equation [13], the generalized Zakharov equations [14], the Chen–Lee–Lin equation [15], and the well-known nonlinear Schrödinger equation [16].

In mathematics and physics, a nonlinear partial differential equation is a partial differential equation with nonlinear components [17]. They have been used to solve mathematical problems such as the Poincaré conjecture and the Calabi–Yau conjecture, as well as to explain a broad range of physical phenomena such as gravity and fluid dynamics [18,19]. These are difficult to study since there are no general procedures that apply to all of these equations; instead, each one must be examined as a standalone issue [20]. Nonlinear and linear partial differential equations are distinguished by the features of the operator that defines the PDE [21].

All solutions to a PDE should ideally be wholly specified, which is possible for sure uncommon PDEs [22]. If the equation has a large symmetry group [23], a finite-dimensional compact manifold, perhaps with singularities, may be created. In this situation, the moduli space of solutions modulo the symmetry group [24] is all that matters. The moduli space may be explicitly compactified in the self-dual Yang–Mills equations, which are somewhat more complicated since the moduli space is finite-dimensional but not necessarily compact [25]. In totally integrable models, where the solutions are often a superposition of solitons, it is occasionally possible to describe all solutions [26]. For example, consider the Korteweg–De Vries equation. Many outstanding solutions may be stated as fundamental functions [27]. Ordinary differential equations, typically solved correctly, are a helpful place to start when looking for straightforward solutions to complicated problems [28–30].

Mathematical Analysis of Model

This paper studies the $\mathcal{RR}$ equation which is given by [31,32]

$$\mathcal{R}_{xt} - r_1\,\mathcal{R}_{xx} + \mathcal{R} + i\,r_2\,|\mathcal{R}|^2\,\mathcal{R}_x = 0, \tag{4}$$

where $\mathcal{R} = \mathcal{R}(x,t)$ represents a complex smooth envelope function of a spatial variable x and a temporal variable t; r_1, r_2 are real constants. Using the next transformation $\mathcal{R}(x,t) = e^{i\,\psi(\mathfrak{Z})}\,e^{-i\,t\,\omega}\,\varphi(\mathfrak{Z})$, $\mathfrak{Z} = x - \lambda\,t$ to Equation (4), we obtain

$$\begin{cases} \text{Re:} & (-\lambda - r_1)\varphi'' + \varphi(\lambda + r_1)(\psi')^2 - r_2\varphi^3\psi' + \varphi\omega\psi' + \varphi = 0, \\ \text{Im:} & -\varphi'\left(2(\lambda + r_1)\psi' - r_2\varphi^2 + \omega\right) - \varphi(\lambda + r_1)\psi'' = 0. \end{cases} \tag{5}$$

Substituting $\psi = \int \frac{\left(r_2\varphi(x)^2 - \omega\right)^2}{4r_2(\lambda + r_1)\varphi(x)^2}\,dx$ into the first equation of (5), leads to

$$\left(-16\lambda^2 r_2^2 - 32\lambda r_1 r_2^2 - 16 r_1^2 r_2^2\right)\varphi^3\varphi'' + \varphi^4\left(16\lambda r_2^2 - 6r_2^2\omega^2 + 16 r_1 r_2^2\right) + 8 r_2^3\omega\varphi^6 - 3r_2^4\varphi^8 + \omega^4 = 0. \tag{6}$$

Balancing the terms of Equation (6) by using the homogeneous balance rule and the suggested computational schemes' auxiliary equations $\Big[\mathcal{F}'(\mathfrak{Z}) = \mathcal{J}_3\,\mathcal{F}(\mathfrak{Z})^2 + \mathcal{J}_2\,\mathcal{F}(\mathfrak{Z}) + \mathcal{J}_1 \mapsto (\text{ExD method } [33])\,\&\,\mathcal{G}'(\mathfrak{Z}) = \mathcal{G}(\mathfrak{Z})^2 + \varrho \mapsto (\text{ImFE method } [34])\,\&\,\mathscr{B}'(\mathfrak{Z}) = \ln(\mathcal{K})\left(\mathscr{B}(\mathfrak{Z})^2 - \mathscr{B}(\mathfrak{Z})\right) \mapsto (\text{MKud method } [35])\Big]$, where $\mathcal{J}_1$, $\mathcal{J}_2$, $\mathcal{J}_3$, ϱ, a are arbitrary constants, lead to $N = \frac{1}{2}$. Consequently, we have to use another transformation that is given by $\varphi(\mathfrak{Z}) = \sqrt{\mathcal{Y}(\mathfrak{Z})}$. Thus, Equation (6) transforms into the following formula

$$\mathcal{Y}\mathcal{Y}'' + \mathcal{Y}^4\mathcal{L}_2 - \mathcal{Y}^3\mathcal{L}_3 - \mathcal{Y}^2\mathcal{L}_4 - \mathcal{L}_1(\mathcal{Y}')^2 + \mathcal{L}_5 = 0, \tag{7}$$

where $\left[\mathcal{L}_1 = \frac{1}{2},\ \mathcal{L}_2 = \frac{3r_2^2}{8(\lambda+r_1)^2},\ \mathcal{L}_3 = \frac{r_2\omega}{(\lambda+r_1)^2},\ \mathcal{L}_4 = \frac{8\lambda+8r_1-3\omega^2}{4(\lambda+r_1)^2},\ \mathcal{L}_5 = -\frac{\omega^4}{8r_2^2(\lambda+r_1)^2}\right]$. Using the homogeneous balance rule on Equation (7), leads to $N = 1$. Thus, the general solutions of the suggested model through the above-mentioned computational schemes are formulated by (for more detial about the implemented schemes; see (Appendix A):

$$\mathcal{Y}(\mathfrak{Z}) = \begin{cases} \sum_{i=0}^{n} a_i\, \mathcal{F}(\mathfrak{Z})^i = a_1\, \mathcal{F}(\mathfrak{Z}) + a_0, \\ \sum_{i=0}^{n} a_i\, (\mathcal{G}(\mathfrak{Z}) + \mu)^i = a_1(\mu + \mathcal{G}(\mathfrak{Z})) + a_0, \\ \sum_{i=0}^{n} a_i\, \mathcal{B}(\mathfrak{Z})^i = a_1\, \mathcal{B}(\mathfrak{Z}) + a_0, \end{cases} \tag{8}$$

where a_0, a_1 are arbitrary constants to be evaluated through the methods' frameworks.

The rest paper's sections are given in the following order; novel solitary wave solutions of the investigated model and their numerical simulations are given in Section 2. The paper's contributions are given in Section 3. The summary of our study and its results are summarized in Section 4.

2. Solitary Wave Solutions

This section aims to derive some novel solitary wave solutions to the $\mathcal{RR}$ equation using the above-suggested computational schemes. Furthermore, the constructed solutions are represented through contour, two-dimensional, and three-dimensional graphs to illustrate the pulses' propagation in optical fibers.

2.1. The ExD Method's Results

Investigating the above-parameters' values through the ExD method's framework, leads to

Set I

$$\mathcal{L}_1 \to \frac{1}{2}, \mathcal{L}_2 \to -\frac{3\mathcal{J}_3^2}{2a_1^2}, \mathcal{L}_3 \to \frac{2\mathcal{J}_3(a_1\mathcal{J}_2 - 2a_0\mathcal{J}_3)}{a_1^2}, \mathcal{L}_4 \to \frac{3a_0\mathcal{J}_3(a_0\mathcal{J}_3 - a_1\mathcal{J}_2)}{a_1^2} + \frac{\mathcal{J}_2^2}{2} + \mathcal{J}_1\mathcal{J}_3,$$
$$\mathcal{L}_5 \to \frac{\left(a_0^2\mathcal{J}_3 - a_1a_0\mathcal{J}_2 + a_1^2\mathcal{J}_1\right)^2}{2a_1^2}.$$

Set II

$$a_0 \to 0, a_1 \to i\sqrt{\frac{3}{2}}\frac{\mathcal{J}_3}{\sqrt{\mathcal{L}_2}}, \mathcal{L}_1 \to \frac{1}{2}, \mathcal{L}_3 \to -2i\sqrt{\frac{2}{3}}\mathcal{J}_2\sqrt{\mathcal{L}_2}, \mathcal{L}_4 \to \frac{\mathcal{J}_2^2}{2} + \mathcal{J}_1\mathcal{J}_3, \mathcal{L}_5 \to -\frac{3\mathcal{J}_1^2\mathcal{J}_3^2}{4\mathcal{L}_2},$$

where $(\mathcal{L}_2 < 0)$.

Set III

$$a_1 \to i\sqrt{\frac{3}{2}}\frac{\mathcal{J}_3}{\sqrt{\mathcal{L}_2}}, \mathcal{L}_1 \to \frac{1}{2}, \mathcal{L}_3 \to \frac{2}{3}\left(4a_0\mathcal{L}_2 - i\sqrt{6}\mathcal{J}_2\sqrt{\mathcal{L}_2}\right), \mathcal{L}_4 \to i\sqrt{6}a_0\mathcal{J}_2\sqrt{\mathcal{L}_2} - 2a_0^2\mathcal{L}_2 + \frac{\mathcal{J}_2^2}{2} + \mathcal{J}_1\mathcal{J}_3,$$
$$\mathcal{L}_5 \to \frac{1}{12\mathcal{L}_2}\left(4i\sqrt{6}a_0^3\mathcal{J}_2\mathcal{L}_2^{3/2} + 6a_0^2\left(\mathcal{J}_2^2 + 2\mathcal{J}_1\mathcal{J}_3\right)\mathcal{L}_2 - 6i\sqrt{6}a_0\mathcal{J}_1\mathcal{J}_2\mathcal{J}_3\sqrt{\mathcal{L}_2} - 4a_0^4\mathcal{L}_2^2 - 9\mathcal{J}_1^2\mathcal{J}_3^2\right),$$

where $(\mathcal{L}_2 < 0)$.

Thus, the solitary wave solutions of the investigated model are given by;

For $\mathcal{J}_2 = 0$, $\mathcal{J}_1\mathcal{J}_3 < 0$, we obtain

$$\mathscr{R}_{\mathrm{I},1}(x,t) = \Xi\left(a_0 + \frac{a_1\sqrt{-\mathcal{J}_1\mathcal{J}_3}\,\tanh\left(\sqrt{-\mathcal{J}_1\mathcal{J}_3}(x-\lambda\,t) + \frac{\log(\vartheta)}{2}\right)}{\mathcal{J}_3}\right)^{\frac{1}{2}}, \tag{9}$$

$$\mathscr{R}_{\mathrm{I},2}(x,t) = \Xi\left(a_0 + \frac{a_1\sqrt{-\mathcal{J}_1\mathcal{J}_3}\,\coth\left(\sqrt{-\mathcal{J}_1\mathcal{J}_3}(x-\lambda\,t) + \frac{\log(\vartheta)}{2}\right)}{\mathcal{J}_3}\right)^{\frac{1}{2}}, \tag{10}$$

$$\mathscr{R}_{\mathrm{II},1}(x,t) = \Xi\left(\frac{i\sqrt{\frac{3}{2}}\sqrt{-\mathcal{J}_1\mathcal{J}_3}\,\tanh\left(\sqrt{-\mathcal{J}_1\mathcal{J}_3}(x-\lambda\,t) + \frac{\log(\vartheta)}{2}\right)}{\sqrt{\mathcal{L}_2}}\right)^{\frac{1}{2}}, \tag{11}$$

$$\mathscr{R}_{\mathrm{II},2}(x,t) = \Xi\left(\frac{i\sqrt{\frac{3}{2}}\sqrt{-\mathcal{J}_1\mathcal{J}_3}\,\coth\left(\sqrt{-\mathcal{J}_1\mathcal{J}_3}(x-\lambda\,t) + \frac{\log(\vartheta)}{2}\right)}{\sqrt{\mathcal{L}_2}}\right)^{\frac{1}{2}}, \tag{12}$$

$$\mathscr{R}_{\mathrm{III},1}(x,t) = \Xi\left(a_0 + \frac{i\sqrt{\frac{3}{2}}\sqrt{-\mathcal{J}_1\mathcal{J}_3}\,\tanh\left(\sqrt{-\mathcal{J}_1\mathcal{J}_3}(x-\lambda\,t) + \frac{\log(\vartheta)}{2}\right)}{\sqrt{\mathcal{L}_2}}\right)^{\frac{1}{2}}, \tag{13}$$

$$\mathscr{R}_{\mathrm{III},2}(x,t) = \Xi\left(a_0 + \frac{i\sqrt{\frac{3}{2}}\sqrt{-\mathcal{J}_1\mathcal{J}_3}\,\coth\left(\sqrt{-\mathcal{J}_1\mathcal{J}_3}(x-\lambda\,t) + \frac{\log(\vartheta)}{2}\right)}{\sqrt{\mathcal{L}_2}}\right)^{\frac{1}{2}}. \tag{14}$$

For $\mathcal{J}_1 = 0$, $\mathcal{J}_2 > 0$, we obtain

$$\mathscr{R}_{\mathrm{I},3}(x,t) = \Xi\left(a_0 + \frac{a_1\mathcal{J}_2\,e^{\mathcal{J}_2(-\lambda\,t+x+\vartheta)}}{1-\mathcal{J}_3e^{\mathcal{J}_2(-\lambda\,t+x+\vartheta)}}\right)^{\frac{1}{2}}, \tag{15}$$

$$\mathscr{R}_{\mathrm{II},3}(x,t) = \Xi\left(-\frac{i\sqrt{\frac{3}{2}}\mathcal{J}_2\mathcal{J}_3\,e^{\mathcal{J}_2(-\lambda\,t+x+\vartheta)}}{\sqrt{\mathcal{L}_2}\left(\mathcal{J}_3e^{\mathcal{J}_2(-\lambda\,t+x+\vartheta)}-1\right)}\right)^{\frac{1}{2}}, \tag{16}$$

$$\mathscr{R}_{\mathrm{III},3}(x,t) = \Xi\left(a_0 - \frac{i\sqrt{\frac{3}{2}}\mathcal{J}_2\mathcal{J}_3\,e^{\mathcal{J}_2(-\lambda\,t+x+\vartheta)}}{\sqrt{\mathcal{L}_2}\left(\mathcal{J}_3e^{\mathcal{J}_2(-\lambda\,t+x+\vartheta)}-1\right)}\right)^{\frac{1}{2}}. \tag{17}$$

For $\mathcal{J}_1 = 0$, $\mathcal{J}_2 < 0$, we obtain

$$\mathscr{R}_{\mathrm{I},4}(x,t) = \Xi\left(a_0 - a_1 + \frac{a_1}{\mathcal{J}_3e^{\mathcal{J}_2(-\lambda\,t+x+\vartheta)}+1}\right)^{\frac{1}{2}}, \tag{18}$$

$$\mathscr{R}_{\mathrm{II},4}(x,t) = \Xi\left(-\frac{i\sqrt{\frac{3}{2}}\mathcal{J}_3^2\, e^{\mathcal{J}_2(-\lambda\, t+x+\vartheta)}}{\sqrt{\mathcal{L}_2}\left(\mathcal{J}_3 e^{\mathcal{J}_2(-\lambda\, t+x+\vartheta)}+1\right)}\right)^{\frac{1}{2}}, \tag{19}$$

$$\mathscr{R}_{\mathrm{III},4}(x,t) = \Xi\left(a_0 - \frac{i\sqrt{\frac{3}{2}}\mathcal{J}_3^2\, e^{\mathcal{J}_2(-\lambda\, t+x+\vartheta)}}{\sqrt{\mathcal{L}_2}\left(\mathcal{J}_3 e^{\mathcal{J}_2(-\lambda\, t+x+\vartheta)}+1\right)}\right)^{\frac{1}{2}}. \tag{20}$$

For $4\mathcal{J}_1\mathcal{J}_3 > \mathcal{J}_2^2$, we get

$$\mathscr{R}_{\mathrm{I},5}(x,t) = \Xi\left(-\frac{a_1\mathcal{J}_2}{2\mathcal{J}_3} + a_0 + \frac{a_1\sqrt{4\mathcal{J}_1\mathcal{J}_3-\mathcal{J}_2^2}\,\tan\left(\frac{1}{2}\sqrt{4\mathcal{J}_1\mathcal{J}_3-\mathcal{J}_2^2}(-\lambda\, t+x+\vartheta)\right)}{2\mathcal{J}_3}\right)^{\frac{1}{2}}, \tag{21}$$

$$\mathscr{R}_{\mathrm{I},6}(x,t) = \Xi\left(-\frac{a_1\mathcal{J}_2}{2\mathcal{J}_3} + a_0 + \frac{a_1\sqrt{4\mathcal{J}_1\mathcal{J}_3-\mathcal{J}_2^2}\,\cot\left(\frac{1}{2}\sqrt{4\mathcal{J}_1\mathcal{J}_3-\mathcal{J}_2^2}(-\lambda\, t+x+\vartheta)\right)}{2\mathcal{J}_3}\right)^{\frac{1}{2}}, \tag{22}$$

$$\mathscr{R}_{\mathrm{II},5}(x,t) = \Xi\left(\frac{i\sqrt{\frac{3}{2}}\sqrt{4\mathcal{J}_1\mathcal{J}_3-\mathcal{J}_2^2}\,\tan\left(\frac{1}{2}\sqrt{4\mathcal{J}_1\mathcal{J}_3-\mathcal{J}_2^2}(-\lambda\, t+x+\vartheta)\right)}{2\sqrt{\mathcal{L}_2}} - \frac{i\sqrt{\frac{3}{2}}\mathcal{J}_2}{2\sqrt{\mathcal{L}_2}}\right)^{\frac{1}{2}}, \tag{23}$$

$$\mathscr{R}_{\mathrm{II},6}(x,t) = \Xi\left(\frac{i\sqrt{\frac{3}{2}}\sqrt{4\mathcal{J}_1\mathcal{J}_3-\mathcal{J}_2^2}\,\cot\left(\frac{1}{2}\sqrt{4\mathcal{J}_1\mathcal{J}_3-\mathcal{J}_2^2}(-\lambda\, t+x+\vartheta)\right)}{2\sqrt{\mathcal{L}_2}} - \frac{i\sqrt{\frac{3}{2}}\mathcal{J}_2}{2\sqrt{\mathcal{L}_2}}\right)^{\frac{1}{2}}, \tag{24}$$

$$\mathscr{R}_{\mathrm{III},5}(x,t) = \Xi\left(a_0 - \frac{i\sqrt{\frac{3}{2}}\mathcal{J}_2}{2\sqrt{\mathcal{L}_2}} + \frac{i\sqrt{\frac{3}{2}}\sqrt{4\mathcal{J}_1\mathcal{J}_3-\mathcal{J}_2^2}\,\tan\left(\frac{1}{2}\sqrt{4\mathcal{J}_1\mathcal{J}_3-\mathcal{J}_2^2}(-\lambda\, t+x+\vartheta)\right)}{2\sqrt{\mathcal{L}_2}}\right)^{\frac{1}{2}}, \tag{25}$$

$$\mathscr{R}_{\mathrm{III},6}(x,t) = \Xi\left(a_0 - \frac{i\sqrt{\frac{3}{2}}\mathcal{J}_2}{2\sqrt{\mathcal{L}_2}} + \frac{i\sqrt{\frac{3}{2}}\sqrt{4\mathcal{J}_1\mathcal{J}_3-\mathcal{J}_2^2}\,\cot\left(\frac{1}{2}\sqrt{4\mathcal{J}_1\mathcal{J}_3-\mathcal{J}_2^2}(-\lambda\, t+x+\vartheta)\right)}{2\sqrt{\mathcal{L}_2}}\right)^{\frac{1}{2}}. \tag{26}$$

where $\Xi = \exp\left(\frac{i}{4\, r_2\,(\lambda+r_1)}\int \frac{\left(\omega - r_2\,\varphi^2\right)^2}{\varphi^2}\, d\,\mathfrak{Z} - i\, t\omega\right)$.

2.2. The ImFE Method's Results

Investigating the above-parameters' values through the ImFE method's framework, leads to

Set I

$$\mathcal{L}_1 \to \frac{1}{2}, \mathcal{L}_2 \to -\frac{3}{2a_1^2}, \mathcal{L}_3 \to -\frac{4(a_1\mu + a_0)}{a_1^2}, \mathcal{L}_4 \to \frac{3a_0(2a_1\mu + a_0)}{a_1^2} + 3\mu^2 + \varrho,$$
$$\mathcal{L}_5 \to \frac{\left(a_1^2(\mu^2 + \varrho) + 2a_1a_0\mu + a_0^2\right)^2}{2a_1^2}.$$

Set II

$$a_0 \to -\frac{1}{4}a_1(a_1\mathcal{L}_3 + 4\mu), \mathcal{L}_1 \to \frac{1}{2}, \mathcal{L}_2 \to -\frac{3}{2a_1^2}, \mathcal{L}_4 \to \frac{1}{8}a_1^2\mathcal{L}_3^2 - \frac{\sqrt{2}\sqrt{\mathcal{L}_5}}{a_1}, \varrho \to -\frac{1}{16}a_1^2\mathcal{L}_3^2 - \frac{\sqrt{2}\sqrt{\mathcal{L}_5}}{a_1}.$$

Thus, the solitary wave solutions of the investigated model are given by
For $\varrho \neq 0$, we obtain

$$\mathscr{R}_{\mathrm{I},1}(x,t) = \Xi\left(a_1(\mu + \sqrt{\varrho}\tan(\sqrt{\varrho}\,(x - \lambda\, t))) + a_0\right)^{\frac{1}{2}}, \tag{27}$$

$$\mathscr{R}_{\mathrm{I},2}(x,t) = \Xi\left(a_1(\mu - \sqrt{\varrho}\cot(\sqrt{\varrho}\,(x - \lambda\, t))) + a_0\right)^{\frac{1}{2}}, \tag{28}$$

$$\mathscr{R}_{\mathrm{II},1}(x,t) = \Xi\left(-\frac{1}{4}a_1\left(a_1\mathcal{L}_3 - 4\sqrt{\varrho}\tan(\sqrt{\varrho}\,(x - \lambda\, t))\right)\right)^{\frac{1}{2}}, \tag{29}$$

$$\mathscr{R}_{\mathrm{II},2}(x,t) = \Xi\left(-\frac{1}{4}a_1\left(a_1\mathcal{L}_3 + 4\sqrt{\varrho}\cot(\sqrt{\varrho}\,(x - \lambda\, t))\right)\right)^{\frac{1}{2}}. \tag{30}$$

For $\varrho = 0$, we obtain

$$\mathscr{R}_{\mathrm{I},3}(x,t) = \Xi\left(a_1\left(\mu + \frac{1}{\lambda\, t - x}\right) + a_0\right)^{\frac{1}{2}}, \tag{31}$$

$$\mathscr{R}_{\mathrm{II},4}(x,t) = \Xi\left(\frac{1}{4}a_1\left(-a_1\mathcal{L}_3 - \frac{4}{x - \lambda\, t}\right)\right)^{\frac{1}{2}}. \tag{32}$$

where $\Xi = \exp\left(\frac{i}{4r_2\,(\lambda + r_1)}\int \frac{\left(\omega - r_2\,\varphi^2\right)^2}{\varphi^2}\,d\,\mathfrak{Z} - i\,t\omega\right)$.

2.3. The MKud Method's Results

Investigating the above-parameters' values through the ImFE method's framework, leads to

$$\mathcal{L}_1 \to \frac{1}{2}, \mathcal{L}_2 \to -\frac{3\ln^2(\mathcal{K})}{2a_1^2}, \mathcal{L}_3 \to -\frac{2(2a_0 + a_1)\ln^2(\mathcal{K})}{a_1^2}, \mathcal{L}_4 \to \frac{\left(6a_0^2 + 6a_1a_0 + a_1^2\right)\ln^2(\mathcal{K})}{2a_1^2},$$
$$\mathcal{L}_5 \to \frac{a_0^2(a_0 + a_1)^2\ln^2(\mathcal{K})}{2a_1^2}.$$

Thus , the solitary wave solutions of the investigated model are given by

$$\mathcal{R}(x,t) = \Xi \left(\frac{a_1}{1 \pm \mathcal{K}^{(x-\lambda\, t)}} + a_0 \right)^{\frac{1}{2}}. \tag{33}$$

where $\Xi = \exp\left(\frac{i}{4\, r_2\, (\lambda + r_1)} \int \frac{\left(\omega - r_2\, \varphi^2\right)^2}{\varphi^2}\, d\,\mathfrak{Z} - i\, t\omega \right)$.

3. Results and Discussion

This section investigates the paper's results and the employed computational schemes. Three analytical (ExD, ImFE, and MKud) techniques have been applied to the $\mathcal{RR}$ equation and many soliton wave solutions have been constructed in various formulas. The applied methods' auxiliary equations are similar. The ExD and ImFE methods are equivalent $\mapsto$ $(\mathcal{J}_3 = 1, \mathcal{J}_2 = \varrho, \mathcal{J}_1 = 0)$, the ExD, and MKud methods are equivalent $\mapsto$ $(\mathcal{J}_3 = 1, \mathcal{J}_2 = -1, \mathcal{J}_1 = 0, \mathcal{K} = 10)$, and the ExD, and MKud methods are equivalent $\mapsto$ $(\mathcal{J}_3 = 1, \mathcal{J}_2 = -1, \mathcal{J}_1 = 0, \mathcal{K} = 10)$. This equivalence between the applied computational schemes' auxiliary equations leads to similarity of their methods' solutions, such as Equations (9)–(14), (27)–(30), which are similar to each other but at the same time are different from the previously published articles. Comparing our constructed solutions with those that have been published in [36–38] leads to distinguishing the novelty of our results. The obtained results of Equations (9), (11), (13), (27), and (29) are represented in some graphs (Figures 1–6 where each of these figures contains three distinct representations of the tested solutions and these representations are given, respectively, (a) 3D, (b) 2D, and (c) contour graphs.). These represented figures have the following parameter: Figure 1 uses $(a_0 = 7, a_1 = 6, \mathcal{J}_1 = -3, \mathcal{J}_3 = 27, \mathcal{J}_3 = 5, \lambda = 9, \Xi = 1, \vartheta = 1)$, Figure 2 is given under $(\mathcal{J}_1 = -1, \mathcal{J}_3 = 9, \lambda = 5, \Xi = 1, \mathcal{L}_2 = -4, \vartheta = 1)$, Figure 3 is illustrated for $(a_0 = 7, \mathcal{J}_1 = -1, \mathcal{J}_3 = 4, \lambda = 8, \Xi = 1, \mathcal{L}_2 = -8, \vartheta = 1)$, Figure 4 is demonstrated by $(a_0 = 3, a_1 = 6, \lambda = 8, \mu = 5, \Xi = 1, \varrho = -4)$, Figure 5 is numerically given by $(a_0 = 3, a_1 = 6, \lambda = 5, \Xi = 1, \mathcal{L}_3 = 5, \varrho = -9)$, and Figure 6 is represented by $(a_0 = 3, a_1 = 6, \lambda = 7, \Xi = 1)$. The represented graphs explains some distinct characterizations of the investigated model, respectively: kink wave, singular wave, periodic wave, anti-kink wave, bright, and drak-wave. The interactions between the obtained soliton wave solutions are represented through (Figure 7).

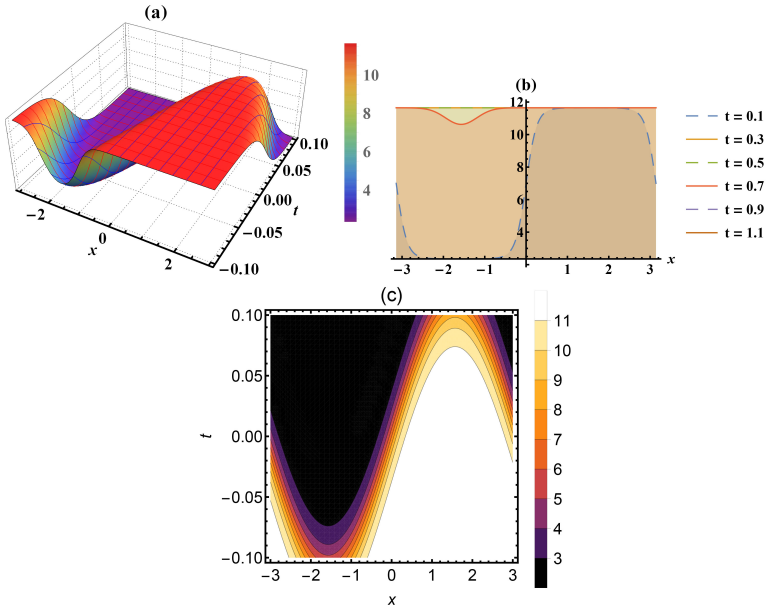

Figure 1. Numerical demonstration of kink waves for Equation (9) in some distinct graphs ((**a**) 3D, (**b**) 2D, and (**c**) density graph).

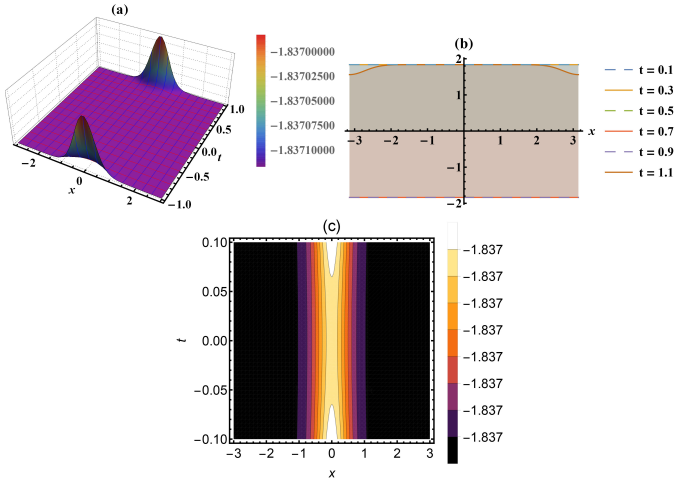

Figure 2. A numerical explanation of kink waves for Equation (11) in some distinct graphs ((**a**) 3D, (**b**) 2D, and (**c**) density graph).

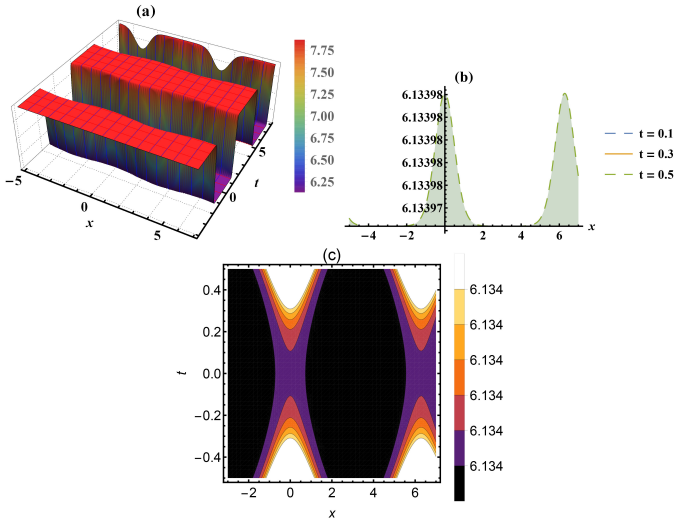

Figure 3. An illustration of periodic kink waves for Equation (13) in some distinct graphs ((**a**) 3D, (**b**) 2D, and (**c**) density graph).

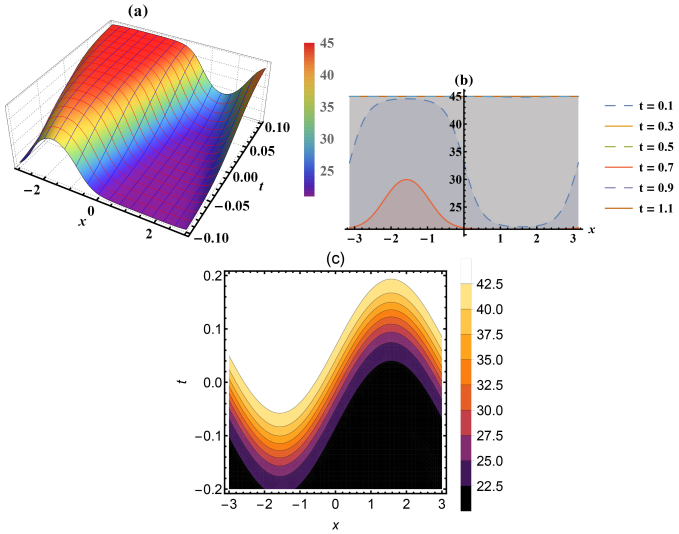

Figure 4. An illustration of kink waves for Equation (27) in some distinct graphs ((**a**) 3D, (**b**) 2D, and (**c**) density graph).

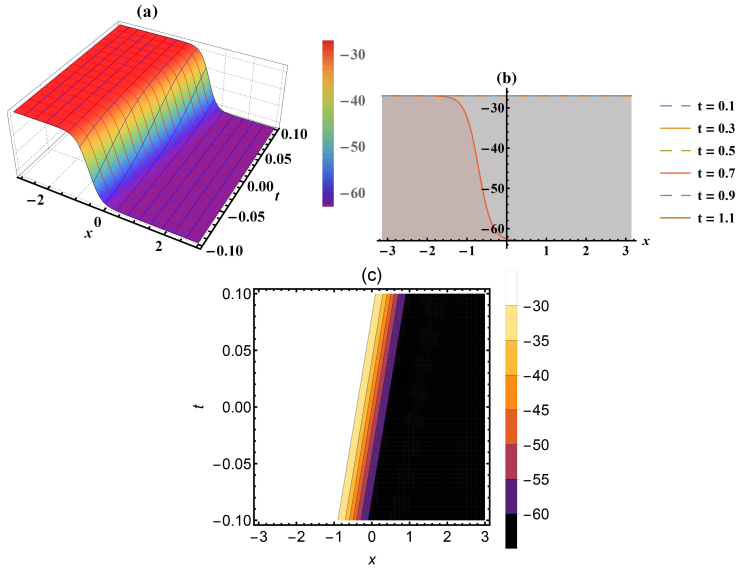

Figure 5. A numerical demonstration of kink waves for Equation (29) in some distinct graphs ((**a**) 3D, (**b**) 2D, and (**c**) density graph).

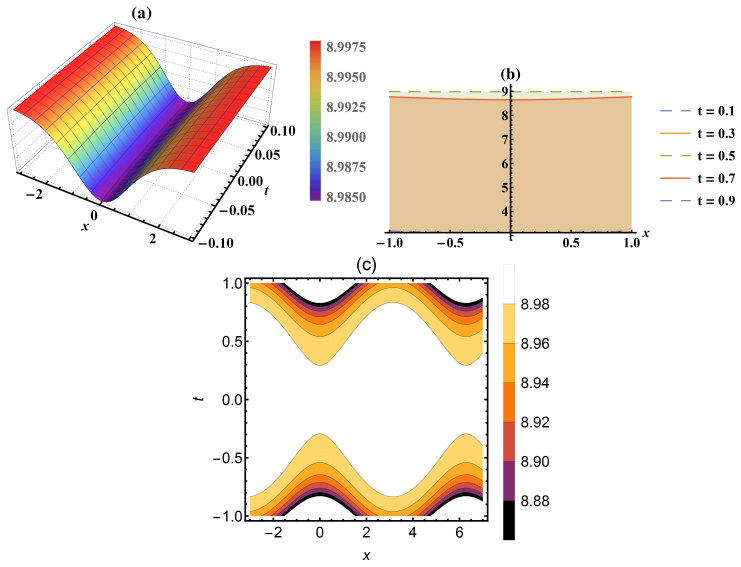

Figure 6. A numerical illustration of periodic kink waves for Equation (33) in some distinct graphs ((**a**) 3D, (**b**) 2D, and (**c**) density graph).

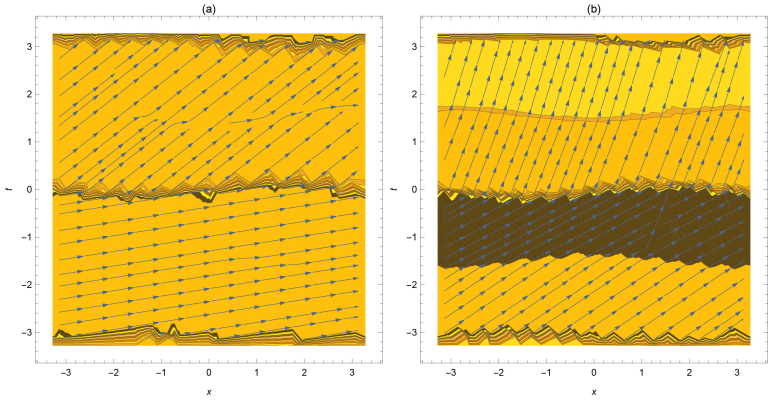

Figure 7. *Cont.*

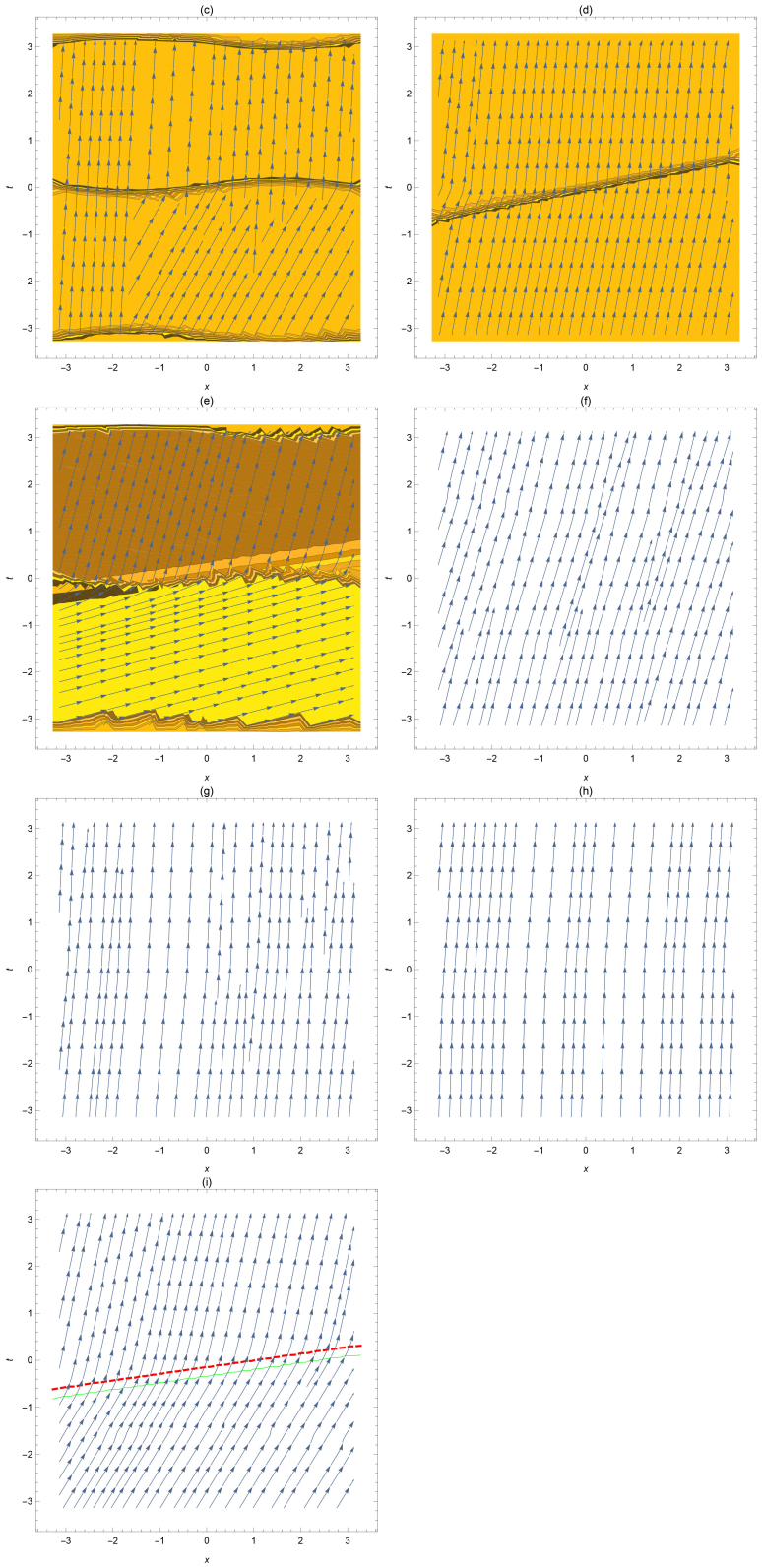

Figure 7. *Cont.*

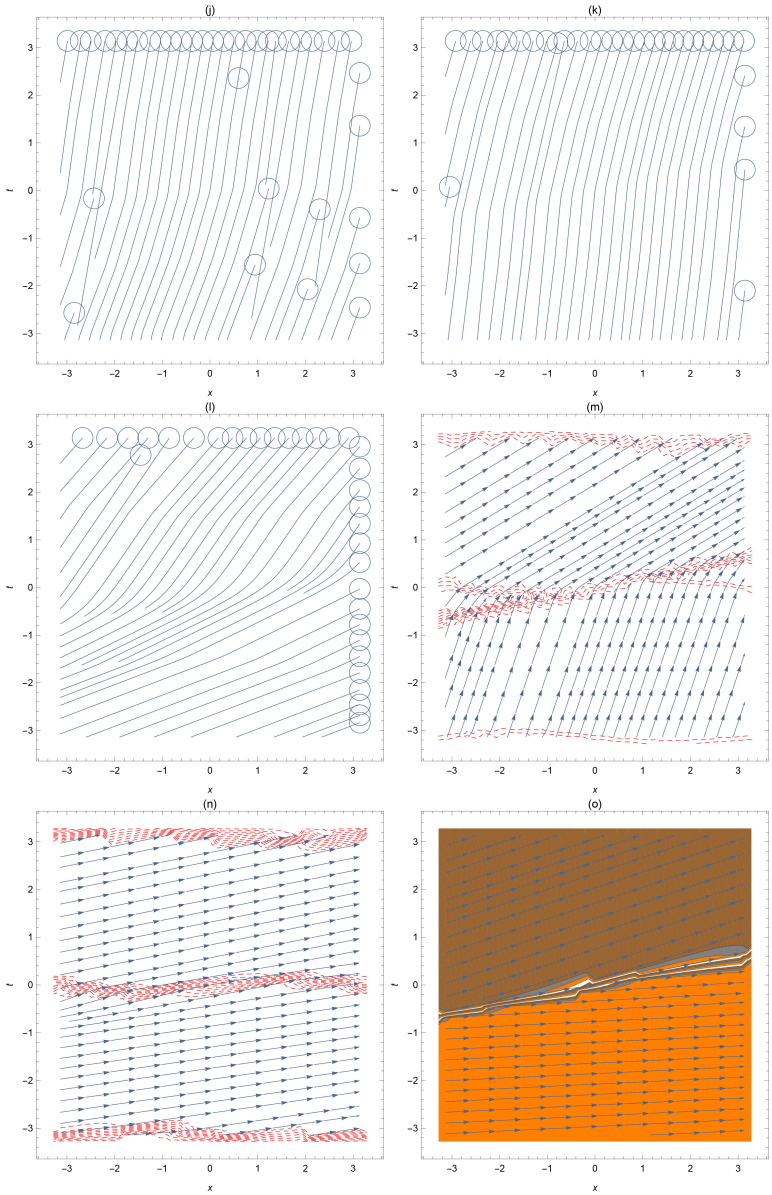

Figure 7. Propagation of pulses regarding the dispersion effect in optical fibers ((**a**) Equation (9), (**b**) Equation (11)). Propagation of pulses regarding the dispersion effect in optical fibers ((**c**) Equation (9), (**d**) Equation (11), (**e**) Equation (13), (**f**) Equation (27), (**g**) Equation (29), (**h**) Equation (33), (**i**) Equation (9)). Propagation of pulses regarding the dispersion effect in optical fibers ((**j**) Equation (9), (**k**) Equation (11), (**l**) Equation (13), (**m**) Equation (27), (**n**) Equation (29), (**o**) Equation (33)).

Finally, studying the above-solutions' stability using the Hamiltonian system characterizations leads to find the momentum of Equation (9) in the following structure

$$\begin{aligned}\mathcal{M} =& \frac{1}{162\lambda}\Big(32400\lambda + 30\lambda\Big(\tanh^{-1}(\tanh(15(\lambda+1))) + \tanh^{-1}(\tanh(15-15\lambda))\Big)\\ &+ \log(1-\tanh(15(\lambda+1))) + \log(\tanh(15(\lambda+1))+1)\\ &- \log(1-\tanh(15-15\lambda)) - \log(\tanh(15-15\lambda)+1)\Big).\end{aligned} \tag{34}$$

Thus, we find

$$\left.\frac{\partial\,\mathcal{M}}{\partial\lambda}\right|_{\lambda=5} = 0.0925925926. \tag{35}$$

Consequently, Equation (9) is table solution in $x \in [-5,5]$, $t \in [-5,5]$. With same technique, we can study the other-obtained solutions' stability conditions.

4. Conclusions

This research paper has constructed many soliton wave solutions of the Rangwala–Rao equation in some distinct formulas such as rational, hyperbolic, and trigonometric. These solutions explain the effect of the integrability conditions on the electric field's slowly varying envelope. Moreover, it impacts the slowly changing electric field envelope and the propagation of pulses in optical fibers regarding the dispersion effect. All these characterizations have been explained through some distinguished graphs. The paper's novelty and scientific contributions have been discussed by comparing our results with previously published articles. All solutions' accuracy has been checked by putting them back into the original model by Mathematica 13.1.

Funding: This research received no external funding.

Data Availability Statement: The data that support the findings of this study are available from the corresponding author upon reasonable request.

Acknowledgments: My sincere thanks go to the journal's editor and to the anonymous reviewers who contributed detailed comments and suggestions to improve the paper.

Conflicts of Interest: This work does not have any conflict of interest.

Appendix A

This section gives the methods' headlines as follows:

Assume the following form for the equation of nonlinear evolution:

$$\mathcal{E}(\mathfrak{U}, \mathfrak{U}_x, \mathfrak{U}_t, \mathfrak{U}_{x,t}, \ldots) = 0, \tag{A1}$$

where $\mathcal{E} = \mathcal{E}(x,t)$ is a polynomial of $\mathfrak{U}(x,t)$ and its partial derivatives wherein the highest order derivatives and nonlinear terms are concerned. The main steps of the employed method [33–35] are as follows

Step 1. The traveling wave transformation

$$\mathfrak{U}(x,\, t) = \nu(\mathfrak{Z}), \quad \mathfrak{Z} = x + c\, t, \tag{A2}$$

converting Equation (A1) into the following ODE

$$\mathcal{E}\left(\nu,\, \nu', \nu'', \ldots\right) = 0, \tag{A3}$$

where $\mathcal{E}$ is a polynomial in $\nu(\mathfrak{Z})$ and its total derivatives, wherein $\nu'(\mathfrak{Z}) = \frac{d\nu}{d\mathfrak{Z}}$.

Step 2. We suppose the solution of (A3) is of the form

$$\nu(\mathfrak{Z}) = \begin{cases} \sum\limits_{i=0}^{N} a_i\, \mathcal{F}(\mathfrak{Z})^i, \\ \sum\limits_{i=0}^{N} a_i\, (\mathcal{G}(\mathfrak{Z}) + \mu)^i, \\ \sum\limits_{i=0}^{N} a_i\, \mathcal{B}(\mathfrak{Z})^i, \end{cases} \tag{A4}$$

where a_k $(k = 0, 1, 2, 3, \ldots, N)$ are arbitrary constants to be determined, such that $a_N \neq 0$, and $\Phi(\mathfrak{Z})$ is an unidentified function to be determined afterwards. This function satisfies the following equation

$$\begin{cases} \mathcal{F}'(\mathfrak{Z}) = \mathcal{J}_3\,\mathcal{F}(\mathfrak{Z})^2 + \mathcal{J}_2\,\mathcal{F}(\mathfrak{Z}) + \mathcal{J}_1, \\ \mathcal{G}'(\mathfrak{Z}) = \mathcal{G}(\mathfrak{Z})^2 + \varrho, \\ \mathcal{B}'(\mathfrak{Z}) = \ln(\mathcal{K})\big(\mathcal{B}(\mathfrak{Z})^2 - \mathcal{B}(\mathfrak{Z})\big), \end{cases} \tag{A5}$$

where $\mathcal{J}_1$, $\mathcal{J}_2$, $\mathcal{J}_3$, ϱ, a are arbitrary constants

Step 3. We determine the positive integer N come out in (A4) by considering the homogeneous balance between the highest order derivatives and the highest order nonlinear terms occurring in (A3).

Step 4. We compute all the required derivatives $v', v'', \ldots$, and substitute (A4) and the derivatives into (A3) and then we account for the function $\mathcal{F}(\mathfrak{Z})$, $\mathcal{G}(\mathfrak{Z})$, $\mathcal{B}(\mathfrak{Z})$. As a result of this substitution, we obtain a polynomial of $\mathcal{F}^j(\mathfrak{Z})$, $\mathcal{G}^j(\mathfrak{Z})$, $\mathcal{B}^j(\mathfrak{Z})$ and its derivatives. In this polynomial, we equate all the coefficients to zero. This procedure yields a system of equations whichever can be solved to find a_k and $\mathcal{F}(\mathfrak{Z})$, $\mathcal{G}(\mathfrak{Z})$, $\mathcal{B}(\mathfrak{Z})$.

References

1. Khater, M.M. Nonlinear biological population model; computational and numerical investigations. *Chaos Solitons Fractals* **2022**, *162*, 112388. [CrossRef]
2. Khater, M.M. Nonparaxial pulse propagation in a planar waveguide with Kerr–like and quintic nonlinearities; computational simulations. *Chaos Solitons Fractals* **2022**, *157*, 111970. [CrossRef]
3. Zhang, J.; Lu, D.; Salama, S.A.; Khater, M.M. Accurate demonstrating of the interactions of two long waves with different dispersion relations: Generalized Hirota–Satsuma couple KdV equation. *AIP Adv.* **2022**, *12*, 025015. [CrossRef]
4. Attia, R.A.M.; Zhang, X.; Khater, M.M.A. Analytical and hybrid numerical simulations for the (2+ 1)-dimensional Heisenberg ferromagnetic spin chain. *Results Phys.* **2022**, *43*, 106045. [CrossRef]
5. Feng, Z. On explicit exact solutions for the Lienard equation and its applications. *Phys. Lett. A* **2002**, *293*, 50–56. [CrossRef]
6. Villari, G. On the qualitative behaviour of solutions of Liénard equation. *J. Differ. Equ.* **1987**, *67*, 269–277. [CrossRef]
7. Islam, M.N.; İlhan, O.A.; Akbar, M.A.; Benli, F.B.; Soybaş, D. Wave propagation behavior in nonlinear media and resonant nonlinear interactions. *Commun. Nonlinear Sci. Numer. Simul.* **2022**, *108*, 106242. [CrossRef]
8. Kengne, E.; Liu, W. Modulational instability and sister chirped femtosecond modulated waves in a nonlinear Schrödinger equation with self-steepening and self-frequency shift. *Commun. Nonlinear Sci. Numer. Simul.* **2022**, *108*, 106240. [CrossRef]
9. Guan, X.; Zhou, Q.; Biswas, A.; Alzahrani, A.K.; Liu, W. Darboux transformation for a generalized Ablowitz-Kaup-Newell-Segur hierarchy equation. *Phys. Lett. A* **2020**, *384*, 126394. [CrossRef]
10. Kudryashov, N.A. Traveling wave solutions of the generalized Gerdjikov–Ivanov equation. *Optik* **2020**, *219*, 165193. [CrossRef]
11. Kaya, D. An implementation of the ADM for generalized one-dimensional Klein-Gordon equation. *Appl. Math. Comput.* **2005**, *166*, 426–433. [CrossRef]
12. Didenkulova, E. Mixed turbulence of breathers and narrowband irregular waves: mKdV framework. *Phys. D Nonlinear Phenom.* **2022**, *432*, 133130. [CrossRef]
13. Mirzazadeh, M.; Yıldırım, Y.; Yaşar, E.; Triki, H.; Zhou, Q.; Moshokoa, S.P.; Ullah, M.Z.; Seadawy, A.R.; Biswas, A.; Belic, M. Optical solitons and conservation law of Kundu–Eckhaus equation. *Optik* **2018**, *154*, 551–557. [CrossRef]
14. Chang, Q.S.; Guo, B.L.; Jiang, H. Finite difference method for generalized Zakharov equations. *Math. Comput.* **1995**, *64*, 537–553. [CrossRef]
15. Tian, H.Y.; Tian, B.; Sun, Y.; Zhang, C.R. Three-component coupled nonlinear Schrödinger system in a multimode optical fiber: Darboux transformation induced via a rank-two projection matrix. *Commun. Nonlinear Sci. Numer. Simul.* **2022**, *107*, 106097. [CrossRef]
16. Dikandé, A.M. On a Model for Nerve Impulse Generation Mediated by Electromechanical Processes. *Braz. J. Phys.* **2022**, *52*, 41. [CrossRef]
17. Omri, M.; Abdel-Aty, A.H.; Abdel-Khalek, S.; Khalil, E.; Khater, M.M. Computational and numerical simulations of nonlinear fractional Ostrovsky equation. *Alex. Eng. J.* **2022**, *61*, 6887–6895. [CrossRef]
18. Attia, R.A.; Tian, J.; Lu, D.; Aguilar, J.F.G.; Khater, M.M. Unstable novel and accurate soliton wave solutions of the nonlinear biological population model. *Arab. J. Basic Appl. Sci.* **2022**, *29*, 19–25. [CrossRef]
19. Khater, M.M.; Muhammad, S.; Al-Ghamdi, A.; Higazy, M. Abundant wave structures of the fractional Benjamin-Ono equation through two computational techniques. *J. Ocean. Eng. Sci.* 2022, *in press*. [CrossRef]

20. Wang, F.; Muhammad, S.; Al-Ghamdi, A.; Higazy, M.; Khater, M.M. In (1+ 1)–dimension; inelastic interaction of long-surface gravity waves of small-amplitude unidirectional propagation. *J. Ocean. Eng. Sci.* 2022, *in press*. [CrossRef]
21. Ma, H.; Wang, F.; Khater, M.M.; Al-Sehemi, A.G.; Pannipara, M.; Al-Hartomy, O.A.; Higazy, M. Dynamical behavior of the long waves on the surface of the water with a small amplitude in none–dimensional nonlinear lattices. *J. Ocean. Eng. Sci.* 2022, *in press*. [CrossRef]
22. Khater, M.M.; Muhammad, S.; Al-Ghamdi, A.; Higazy, M. Novel soliton wave solutions of the vakhnenko–parkes equation arising in the relaxation medium. *J. Ocean. Eng. Sci.* 2022, *in press*. [CrossRef]
23. Khater, M.M.; Lu, D. Diverse Soliton wave solutions of for the nonlinear potential Kadomtsev–Petviashvili and Calogero–Degasperis equations. *Results Phys.* **2022**, *33*, 105116. [CrossRef]
24. Khater, M.M.; Alfalqi, S.; Alzaidi, J.; Salama, S.A.; Wang, F. Plenty of wave solutions to the ill-posed Boussinesq dynamic wave equation under shallow water beneath gravity. *AIMS Math.* **2022**, *7*, 54–81. [CrossRef]
25. Zhao, D.; Lu, D.; Salama, S.A.; Yongphet, P.; Khater, M.M. Novel and accurate solitary wave solutions of the conformable fractional nonlinear Schrödinger equation. *J. Low Freq. Noise Vib. Act. Control.* **2022**, *41*, 488–499. [CrossRef]
26. Khater, M.M. Lax representation and bi-Hamiltonian structure of nonlinear Qiao model. *Mod. Phys. Lett. B* **2022**, *36*, 2150614. [CrossRef]
27. Zhao, D.; Lu, D.; Khater, M.M. Ultra-short pulses generation's precise influence on the light transmission in optical fibers. *Results Phys.* **2022**, *37*, 105411. [CrossRef]
28. Khater, M.M.; Salama, S.A. Semi–analytical and numerical simulations of the modified Benjamin–Bona–Mahony model. *J. Ocean. Eng. Sci.* **2022**, *7*, 264–271. [CrossRef]
29. Khater, M.M. On the dynamics of strong Langmuir turbulence through the five recent numerical schemes in the plasma physics. *Numer. Methods Partial. Differ. Equ.* **2022**, *38*, 719–728. [CrossRef]
30. Zhao, D.; Attia, R.A.; Tian, J.; Salama, S.A.; Lu, D.; Khater, M.M. Abundant accurate analytical and semi-analytical solutions of the positive Gardner–Kadomtsev–Petviashvili equation. *Open Phys.* **2022**, *20*, 30–39. [CrossRef]
31. Peng, M.; Lin, R.; Chen, Y.; Zhang, Z.; Khater, M.M. Qualitative Analysis in a Beddington–DeAngelis Type Predator–Prey Model with Two Time Delays. *Symmetry* **2022**, *14*, 2535. [CrossRef]
32. Rangwala, A.A.; Rao, J.A. Bäcklund transformations, soliton solutions and wave functions of Kaup–Newell and Wadati–Konno–Ichikawa systems. *J. Math. Phys.* **1990**, *31*, 1126–1132. [CrossRef]
33. Khater, M.M.; Anwar, S.; Tariq, K.U.; Mohamed, M.S. Some optical soliton solutions to the perturbed nonlinear Schrödinger equation by modified Khater method. *AIP Adv.* **2021**, *11*, 025130. [CrossRef]
34. Wazwaz, A.M. A reliable modification of Adomian decomposition method. *Appl. Math. Comput.* **1999**, *102*, 77–86. [CrossRef]
35. Al-Qurashi, M.; Rashid, S.; Jarad, F.; Tahir, M.; Alsharif, A.M. New computations for the two-mode version of the fractional Zakharov-Kuznetsov model in plasma fluid by means of the Shehu decomposition method. *AIMS Math.* **2022**, *7*, 2044–2060. [CrossRef]
36. Singh, S.S. Exact solutions of Kundu-Eckhaus equation and Rangwala-Rao equation by reduction to Liénard equation. *Asian J. Math. Phys.* **2016**, *11*, ama0301.
37. Zhang, J.L.; Wang, M.L. Exact solutions to a class of nonlinear Schrödinger-type equations. *Pramana* **2006**, *67*, 1011–1022. [CrossRef]
38. Al-Muhiameed, Z.I.; Abdel-Salam, E.A.B. Generalized Jacobi elliptic function solution to a class of nonlinear Schrödinger-type equations. *Math. Probl. Eng.* **2011**, *2011*. [CrossRef]